

# 1 Quantification of historical landscape change on the foreland of a receding 2 polythermal glacier, Hørbyebreen, Svalbard

3 Marek W. Ewertowski<sup>1</sup>, David J.A. Evans<sup>2</sup>, David H. Roberts<sup>2</sup>, Aleksandra M. Tomczyk<sup>1</sup>,  
4 Wojciech Ewertowski<sup>1</sup>, Krzysztof Pleksot<sup>1</sup>

5 <sup>1</sup>*Faculty of Geographical and Geological Sciences, Adam Mickiewicz University, Poznań, Poland*

6 <sup>2</sup>*Department of Geography, Durham University, Durham, UK*

7  
8 **Abstract:** The assessment of multi-decadal scale change in a polythermal glacial landsystem  
9 in the high-Arctic is facilitated by a quantitative approach that utilises time-series of aerial  
10 photographs, satellite images, digital elevation models and field geomorphological mapping.  
11 The resulting spatio-temporal analysis illustrates a transition from glacial to  
12 proglacial/paraglacial conditions indicating that: (1) the areal coverage of ice between the  
13 maximum LIA extent and 2013 decreased from 29.35 km<sup>2</sup> to 16.07 km<sup>2</sup>, which is a reduction  
14 in the glacierized area in the catchment from 62% to 34%; (2) the ice volume loss in the  
15 proglacial area amounted to 214.9 (+-3%) millions m<sup>3</sup>, which was attributed mostly to melting  
16 of the glacier snout but to a lesser extent the degradation of ice-cored landforms; (3) the  
17 transition from areas formerly covered by glacier ice to ice-cored moraines, glacialfluvial  
18 deposits, and other landforms was the most intense in the period 1990-2013; (4) two end  
19 member scenarios (polythermal glacial landsystem domains) evolve during glacier recession,  
20 each one dictated by the volume of debris in englacial and supraglacial positions, and include  
21 subglacial surfaces (limited englacial and supraglacial debris) related to temperate basal ice,  
22 and ice-cored lateral moraines and moraine-mound complexes (significant supraglacial debris  
23 accumulations) related to marginal cold based ice. An additional assemblage of geometric ridge  
24 networks (discrete or linear englacial and supraglacial debris concentrations) relates to crevasse  
25 and hydrofracture infill branching out from an esker complex and is indicative of either surging  
26 or later rapid release of pressurised meltwater from temperate to cold based parts of the former  
27 glacier snout.

28 **Keywords:** Svalbard, glacial geomorphology, polythermal glacial landsystem, GIS, ice-cored  
29 moraine, Arctic, paraglacial

## 30 31 1. INTRODUCTION

32 Glacial forelands exposed due to glacier recession are among the most dynamic landscapes in  
33 polar and mountainous areas (e.g. Bennett and Evans, 2012; Bennett et al., 2010; Carrivick and  
34 Heckmann, 2017; Staines et al., 2014) and are intensively modified by various  
35 geomorphological processes related to glacial retreat, meltwater activity, and the paraglacial  
36 adjustment of topography (Ballantyne and Benn, 1994; Carrivick and Heckmann, 2017;

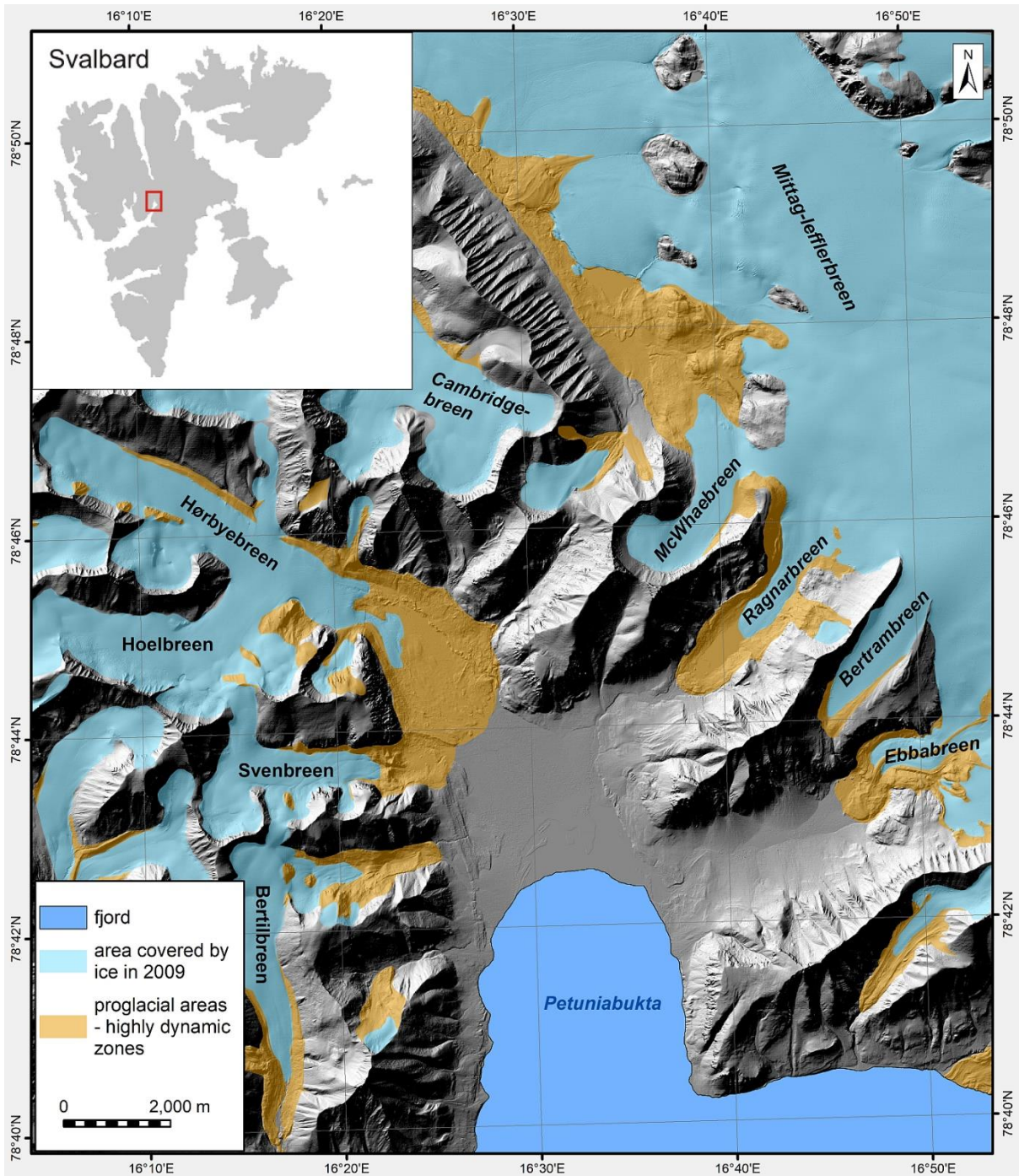
37 Kellerer-Pirklbauer et al., 2010; Kirkbride and Deline, 2018; Mercier et al., 2009; Rachlewicz,  
38 2009; Rachlewicz, 2010). Widespread ice marginal recession in Svalbard since the end of the  
39 Little Ice Age (LIA) has resulted in the exposure of extensive glacier forelands containing a  
40 wide range of glacial landforms, many of which continue to evolve well after deglaciation due  
41 to their significant ice cores. The resulting landform-sediment associations are representative  
42 of the sub-polar glacial landsystem, in many places featuring surge signatures, and their  
43 presently dynamic state provides the ideal opportunity to study changes in glacial process-form  
44 regimes in response to changes in both climatic conditions and geomorphological processes.  
45 Such investigations into the direct connections between processes and forms in contemporary  
46 glacial landscapes allows researchers to compile modern analogues for contextualising  
47 palaeoglaciological reconstructions (cf. Benn and Lukas, 2006; Boulton, 1972; Evans, 2009).  
48 Such investigations also provide a basis for the prediction of future changes in the polar  
49 regions. However, most previous quantitative studies on Svalbard have focused on glaciology  
50 (e.g. Błaszczuk et al., 2013; Hagen and Liestøl, 1990; Hagen et al., 1993; Jania and Hagen,  
51 1996; Lefauconnier and Hagen, 1991; Małecki, 2013; Małecki, 2014; Małecki, 2016; Moholdt  
52 et al., 2010a; Moholdt et al., 2010b; Nuth et al., 2013; Nuth et al., 2010; Rachlewicz et al.,  
53 2007; Sund et al., 2009; Ziaja, 2001; Ziaja, 2005) rather than the ongoing transformations of  
54 proglacial landscapes (e.g. Bennett et al., 2000; Bernard et al., 2016; Lønne and Lyså, 2005;  
55 Lukas et al., 2005; Lyså and Lønne, 2001; Midgley et al., 2013; Schomacker and Kjær, 2008;  
56 Sletten et al., 2001; Strzelecki et al., 2015; Zagorski, 2011; Zagorski et al., 2012; Ziaja, 2004;  
57 Ziaja and Pipała, 2007). Moreover, quantification of the dynamics of landform evolution on  
58 glacier forelands using time-series of digital elevation models or airborne laser scanning has to  
59 date been limited (e.g. Bernard et al., 2016; Etzelmüller, 2000a; Etzelmüller, 2000b; Irvine-  
60 Fynn et al., 2011; Kociuba, 2014; Kociuba, 2016; Kociuba et al., 2014; Midgley et al., 2018;  
61 Tonkin et al., 2016).

62 This study addresses landform transformations on a multi-decadal time-scale on the foreland  
63 of Hørbyebreen, a Svalbard polythermal glacier, in order to assess landscape changes and  
64 glacial landsystem evolution over the last 80 years. The main aim of this study is to characterize  
65 and quantify the deglacial and postglacial transition from glacial to proglacial (paraglacial)  
66 conditions and thereby evaluate spatial and temporal glacial landsystem evolution. The  
67 objectives identified to achieve this aim are: (1) to map and quantify landform development;  
68 and (2) to evaluate the changing patterns of geomorphological processes responsible for  
69 landscape change.

## 70 **2. STUDY AREA**

71 Svalbard is located in the High-Arctic, where continuous permafrost ranges in thickness from  
72 100 m to 500 m (c.f. Etzelmüller and Hagen, 2005; Humlum et al., 2003). The study area is in  
73 the central part of Spitsbergen in the vicinity of Petuniabukta, an area characterised by less ice  
74 cover than most coastal zones due to lower precipitation totals. Around Petuniabukta, an area  
75 of 26 km<sup>2</sup> has been exposed since the termination of LIA as a result of glacier retreat  
76 (Ewertowski and Tomczyk, 2015). Earlier investigations into glaciers and glacial landforms  
77 near Petuniabukta provide a substantial background knowledge of both the geomorphology

78 (e.g. Allaart et al., 2018; Evans et al., 2012; Ewertowski, 2014; Ewertowski et al., 2016;  
 79 Ewertowski et al., 2012; Ewertowski and Tomczyk, 2015; Gibas et al., 2005; Gonera and  
 80 Kasprzak, 1989; Hanáček et al., 2011; Karczewski, 1989; Karczewski et al., 1990; Karczewski  
 81 and Kłysz, 1994; Kłysz, 1985; Křížek et al., 2017; Pleskot, 2015; Rachlewicz, 2009;  
 82 Rachlewicz, 2010; Rachlewicz and Szczuciński, 2008; Stankowski et al., 1989; Strzelecki et  
 83 al., 2018; Strzelecki et al., 2015; Szuman and Kasprzak, 2010), and glaciology (e.g. Małecki,  
 84 2013; Małecki, 2014; Małecki, 2016; Małecki et al., 2013; Rachlewicz, 2009; e.g. Rachlewicz  
 85 et al., 2007), enabling us to link the results of this study to regional changes in the cryosphere.



86  
 87 *Figure 1. Location of the study area.*

88 Hørbyebreen is a valley glacier located at the northern end of Petuniabukta (Figure 1). The  
89 glacier consists of two main flow units, the main unit being named Hørbyebreen and a tributary  
90 unit named Hoelbreen. Its snout is low-lying and surrounded by a large latero-frontal moraine  
91 ridge related to its maximum extent during the LIA. A recent study by Małecki et al. (2013)  
92 found that the glacier was up to 170 m thick and is polythermal, with a temperate 40 m thick  
93 basal layer beneath 100-130 m of polar ice (Małecki et al., 2013). Based on characteristic  
94 features such as a looped medial moraine, Hørbyebreen has been classified as a surge-type  
95 glacier (Farnsworth et al., 2016; Gibas et al., 2005; Karczewski, 1989; Małecki et al., 2013)  
96 but there have been no direct historical observations of any surges by Hørbyebreen. Hence,  
97 other interpretations of the glacier dynamics and associated landsystem signatures have  
98 suggested that Hørbyebreen may instead represent a system that dominated by either: 1)  
99 overprinted polythermal and surging behaviour; or 2) the build-up and rapid intermittent  
100 release of meltwater from the warm-based internal part of a polythermal snout (Evans et al.,  
101 2012).

### 102 3. METHODS

103 Landscape changes in front of Hørbyebreen were quantified using time-series of remote  
104 sensing data (aerial images, satellite images, digital elevation models [DEMs]) and field  
105 geomorphological mapping. Four sets of historical aerial photographs were obtained from the  
106 Norsk Polar Institute. In addition, two sets of satellite images were purchased from Digital  
107 Globe and Apollo mapping companies. In total, the remote sensing data consist of six sets:

- 108 1) Panchromatic oblique frame camera aerial photographs from 1936 and 1938
- 109 2) Panchromatic frame camera photographs from 1961 with a ground pixel size of 0.55 m
- 110 3) Panchromatic frame camera satellite image from Korona satellite from 1965 and 1966
- 111 4) False infrared colour frame camera photographs from 1990 with a ground pixel size of  
112 0.7 m
- 113 5) Colour digital camera photographs from 2009 with a ground resolution of 0.4 m
- 114 6) Multispectral satellite image from Worldview-2 satellite from 2013 with a ground pixel  
115 size 0.5 for panchromatic and 2-m for multispectral bands.

116 Aerial photographs (sets 2, 3 and 4) contained the full camera information and were processed  
117 using photogrammetric software; DEMs and orthophotos were then generated from them. A  
118 total of 16 points, scattered around the glacier snout, were measured in 2012 and 2013 with  
119 Topcon dGPS and used as ground control points for retrospective georeferencing. An  
120 additional 9 points were used as independent control points to assess the quality of the  
121 generated DEMs. The root mean square error (RMSE) in 3D space was calculated from  
122 elevation differences between the DEMs and independent control points: 0.61 m for 1961, 1.25  
123 m for 1990, and 0.95 m for 2009. Additionally, systematic and random vertical errors were  
124 investigated by comparing the 1961 and 1990 DEMs with the 2009 DEM at points where  
125 elevation was expected to be stable (i.e. non-glaciated, non-ice-cored and stable rock areas  
126 expected to undergo very little transformation). These errors were higher than those calculated  
127 from ground-surveyed checkpoints with RMSE of 3.18 for 1961 and 3.40 for 1990; however,

128 their distribution was close to normal, suggesting that errors were random rather than  
129 systematic. Satellite images from 2013 were orthorectified using DEM and ground control  
130 points and then pansharpended.

131 Volumetric transformation of the snout area was calculated from DEMs of differences (DoDs),  
132 (cf. Wheaton et al., 2010). This involves the subtraction of DEMs from each other, enabling  
133 the assessment of spatial and temporal changes, and thus they encompass the two periods 1961-  
134 1990 and 1990-2009. Also important to note is that quantification of transformation of ice and  
135 landform volume changes was restricted only to the mapped part of the glacier snout and not  
136 its entire area. Planimetric transformations were investigated based on all available remote  
137 sensing and field-based data, hence they covered a longer period. Two glacial geomorphology  
138 maps and results of earlier investigations have previously been published (Evans et al., 2012;  
139 Gibas et al., 2005; Karczewski, 1989; Karczewski et al., 1990; Karczewski and Rygielski,  
140 1989; Rachlewicz, 2009; Wojciechowski, 1989), as well as a study concerning changes in  
141 glacial geometry (Małecki et al., 2013) and dynamics (Rachlewicz, 2009). Therefore, we  
142 present new data (including additional maps), with the focus on changes in landforms within  
143 the snout area. Mapping was performed digitally (on-screen vectorisation) and verified during  
144 field campaigns. The projection used in the analysis was UTM zone 33N. All elevation values  
145 provided in the text and figures are ellipsoidal (not above sea level), unless otherwise indicated.

#### 146 **4. RESULTS AND INTERPRETATIONS – SPATIAL AND TEMPORAL** 147 **TRANSFORMATIONS OF GLACIER SNOOT AND ICE-MARGINAL** 148 **(PROGLACIAL) AREA**

149 As a baseline for the results presented here, the 2009 DEM indicates that the elevation of the  
150 glacier ranged from 65 to 695 m a.s.l., and the area classified as the glacier foreland ranged  
151 from 24 to 111 m a.s.l., although the highest ridges of the lateral moraine reached 320 m a.s.l.  
152 The first part of this section provides a brief description of the extent of glacier changes, and  
153 this is followed by an overview of the volumetric and planimetric changes in landforms and  
154 adjacent glacier snout. We then provide a description of the spatial and temporal pattern of  
155 glacial landsystem transformation.

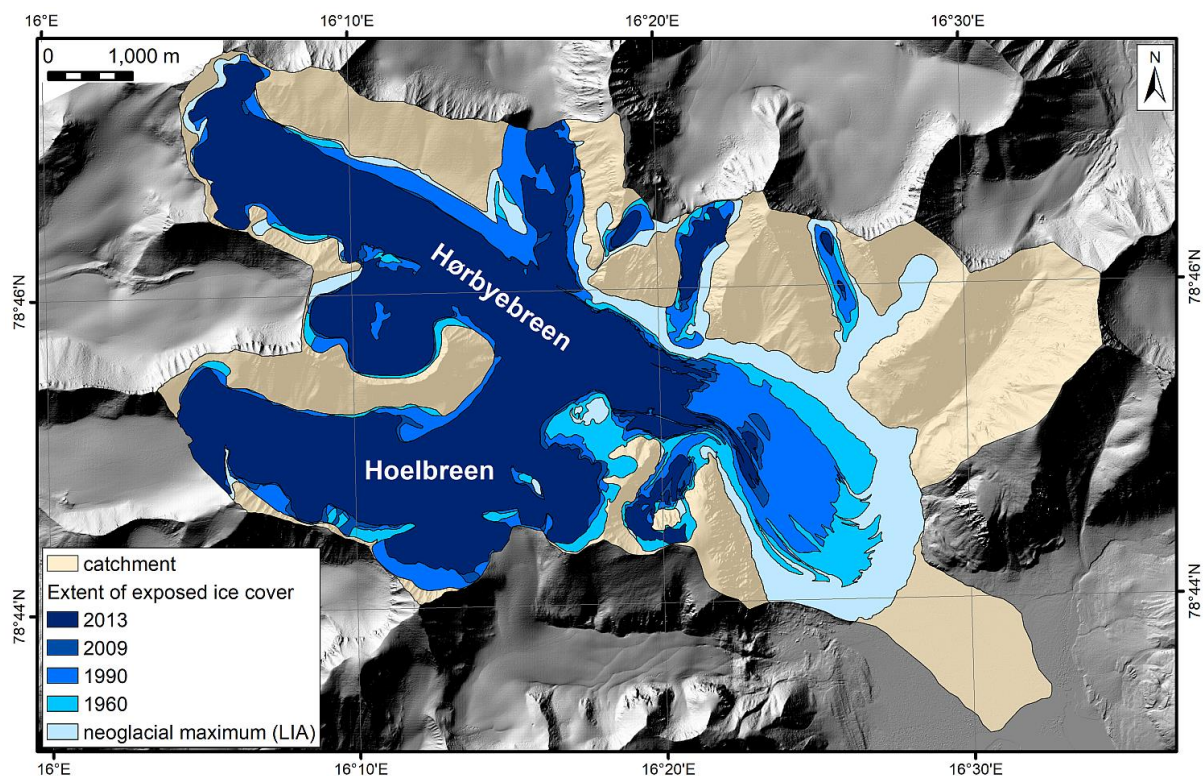
#### 156 **4.1. Glacier changes LIA - 2013**

##### 157 **4.1.1. Glacier extent changes 1900(1920) – 2013**

158 The maximum extent of Hørbyebreen has been delimited using its ice-cored latero-frontal  
159 moraine complex (Evans et al. 2012). It is assumed that the distal slope edges of the moraine  
160 indicate the approximate maximum position of the ice margin. There are no direct data relating  
161 to the timing of this maximum expansion of the snout and therefore we assume that the  
162 recession started around 1900 based upon several studies documenting at least some Svalbard  
163 glaciers having already retreated from their maximum position during the period 1900-1920  
164 (cf. Lamplugh, 1911; Slater, 1925). The extent of the glacier in 1961, 1990, 2009, and 2013  
165 was delimited based on remote sensing data and field verification.



166 The total decrease in the extent of Hørbyebreen for the period 1900 – 2013 was about 13.3 km<sup>2</sup>  
 167 or almost 50% of the maximum extent (Table 1, Figure 2). The presented values indicate the  
 168 change in only the clean glacier cover (i.e. ice surface without debris); there is still a large  
 169 amount of ice buried under the debris of the moraine complex (Evans et al. 2012). Shrinkage  
 170 in the ice cover led to the detachment of three smaller ice units in valleys to the north and one  
 171 to the south, which in the past were linked to the main trunk of the snout (Figure 2). Areas  
 172 provided in Table 1 take into account the total amount of exposed ice cover, including the main  
 173 bodies of Hørbyebreen and Hoelbreen as well as the smaller units now detached and occupying  
 174 higher elevation cirque basins. Since the LIA, the total percentage of the catchment occupied  
 175 by ice decreased from 62% to 34%, which demonstrates the importance of switching from  
 176 glacial to paraglacial geomorphological processes over a very large area.



177

178 *Figure 2. Changes in exposed ice cover from LIA – 2013, Hørbyebreen, Svalbard.*

179

180 The decrease in ice volume was particularly visible in the recession of the glacier snout (Figure  
 181 2), which also varied between the Hoelbreen and Hørbyebreen ice flow units. The distance of  
 182 Hørbyebreen unit snout retreat from the maximum position to the 2013 glacier margin was  
 183 3400 m, representing a mean annual retreat rate of 30 m/year, whereas the Hoelbreen unit snout  
 184 retreated 2000 m or at around 18 m/year. Recent retreat rates (after 1990) were much faster.

185

186 Table. 1. Changes in area of exposed ice cover from LIA – 2013, Hørbyebreen, Svalbard.

year	ice cover [km <sup>2</sup> ]	Ice cover change [%] LIA = 100%	Ice cover percentage of the catchment area (47.61 km <sup>2</sup> ) [%]
<b>LIA</b>	29.35	100	62
<b>1960</b>	24.69	84	52
<b>1990</b>	21.67	74	46
<b>2009</b>	16.83	57	35
<b>2013</b>	16.07	55	34

187

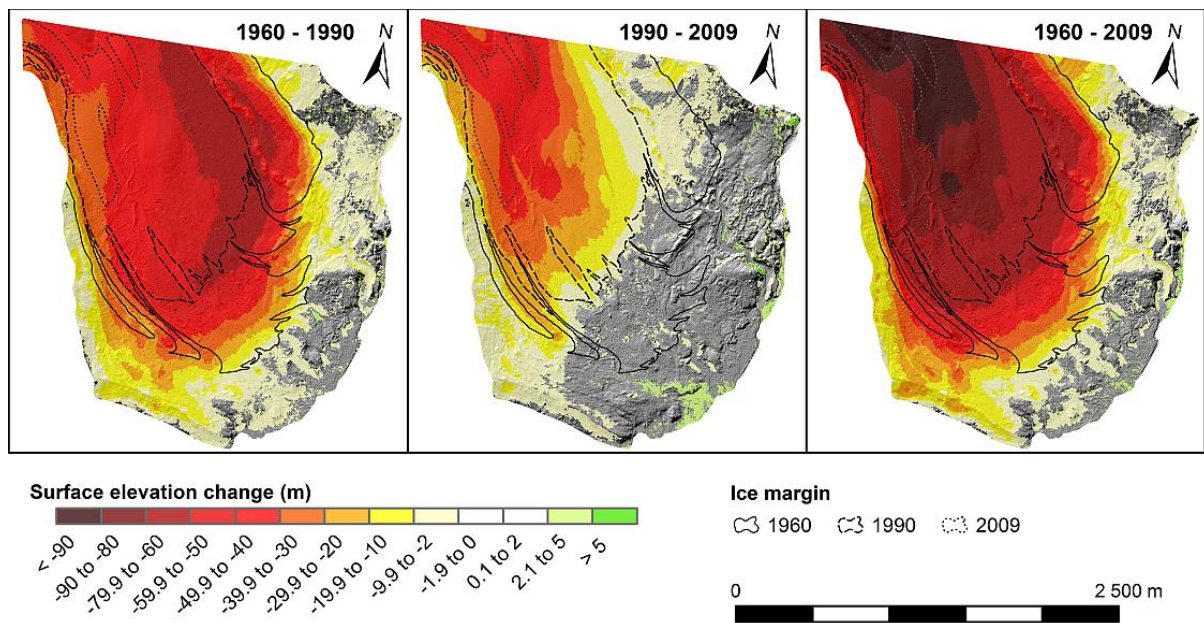
188 **4.1.2. Volume and elevation changes over the glacier snout (1961-2009)**

189 DEM of Differences for the foreland of Hørbyebreen during the periods 1960-1990, 1990-2009  
 190 as well for whole studied period (1960-2009) have shown that widespread lowering is mostly  
 191 related to the melting of the exposed ice surface. Only small areas indicated positive elevation  
 192 changes. The total net volume of change over the 1961-2009 period from the glacier snout and  
 193 foreland was about -215 million m<sup>3</sup> (+/- 3%). Annual percentage changes in snout area and  
 194 volume vary over the study period (Table 2). Spatial variability was different for the two main  
 195 ice flow units, as indicated in the patterns of elevation changes (Figure 3). The total volume  
 196 loss from that part of the latero-frontal which was already exposed in 1960 equalled to 1.8  
 197 million m<sup>3</sup> (+/- 5%) for the period 1960-2009, which translates to a mean volume loss of 0.15  
 198 m/year. This varied significantly, however, from 0 m/year to almost 1.3 m/year depending on  
 199 local topography and the impact of deglacial/paraglacial processes; i.e. most of the  
 200 transformation of latero-frontal ice-cored moraine can be attributed to debris flows and  
 201 backwasting of exposed ice cores (Fig 4 a-c).

202 Data shown in Table 2 and Figure 3 take into account the propagated errors for subsequent  
 203 DEMs. The percentage of the Area of Interest with detectable changes varied from 64% to  
 204 90%, while errors for volume loss were much smaller (from 3 to 8%) than for deposition (from  
 205 62 to 70%) (Table 2). Much larger uncertainty in the measurements of volumes of deposition  
 206 is related to the fact that the increase in surface elevation was usually small (within the range  
 207 of DEM errors).

208 Table 2. Volume changes over the foreland and snout area of Hørbyebreen

Period	Area of loss (m <sup>2</sup> )	Area of deposition (m <sup>2</sup> )	% of Area of Interest with Detectable Changes (%)	Total volume loss (m <sup>3</sup> )	Total volume of deposition (m <sup>3</sup> )	Total net volume differences (m <sup>3</sup> )	Average thickness of volume loss (m)	Average thickness of deposition (m)
1960 - 1990	4 317 648	17 402	89%	152 906 451 (+/- 5%)	48 610 (+/- 67%)	-152 857 841 (+/- 5%)	35	2
1990 - 2009	2 936 321	163 102	64%	62 203 486 (+/- 8%)	407 124 (+/- 70%)	-61 796 363 (+/- 8%)	21	1
Total period (1960 - 2009)	4 310 904	51 572	90%	215 116 548 (+/- 3%)	123 832 (+/- 62%)	-214 992 716 (+/- 3%)	50	2



210

211 Figure 3. Surface elevation change (m) over the snout and proglacial area of Hørbyebreen.

212 Between 1960 and 1990, a larger amount of ice was lost from the Hørbye ice flow unit (NE  
 213 side) compared to a much smaller loss from the Hoel ice flow unit (SW side). Spatial variability  
 214 of ice loss resulted in an increasing asymmetric transverse snout profile over the study period  
 215 (Figure 5). Specifically, the NE side of the glacier snout lowered much more rapidly than the  
 216 SW side. This might relate to various factors such as surge activity and/or high mountain walls  
 217 that effectively reduce the amount of solar energy reaching the southern part of the glacier.  
 218 Conversely, in some place heat radiation from dark rocks resulted in separation of clean ice  
 219 surface from valley sides (Fig. 4d). Spatial variability in glacier snout changes such as this can  
 220 also be interpreted as the product of an uneven distribution of supraglacial debris. On the  
 221 Hoelbreen ice flow unit in particular this is manifest in the occurrence of a thickening debris  
 222 cover that is characterised by prominent longitudinal debris stripes comprising a relatively thin  
 223 (< 10 cm) layer of angular debris (Fig. 4e). The presence of such a thin layer of debris on the  
 224 glacier surface can reduce the ice melt significantly over time (Fig. 4f) (cf. Nakawo and Young,  
 225 1981; Nicholson and Benn, 2006; Nicholson and Benn, 2013; Östrem, 1959).

226

227

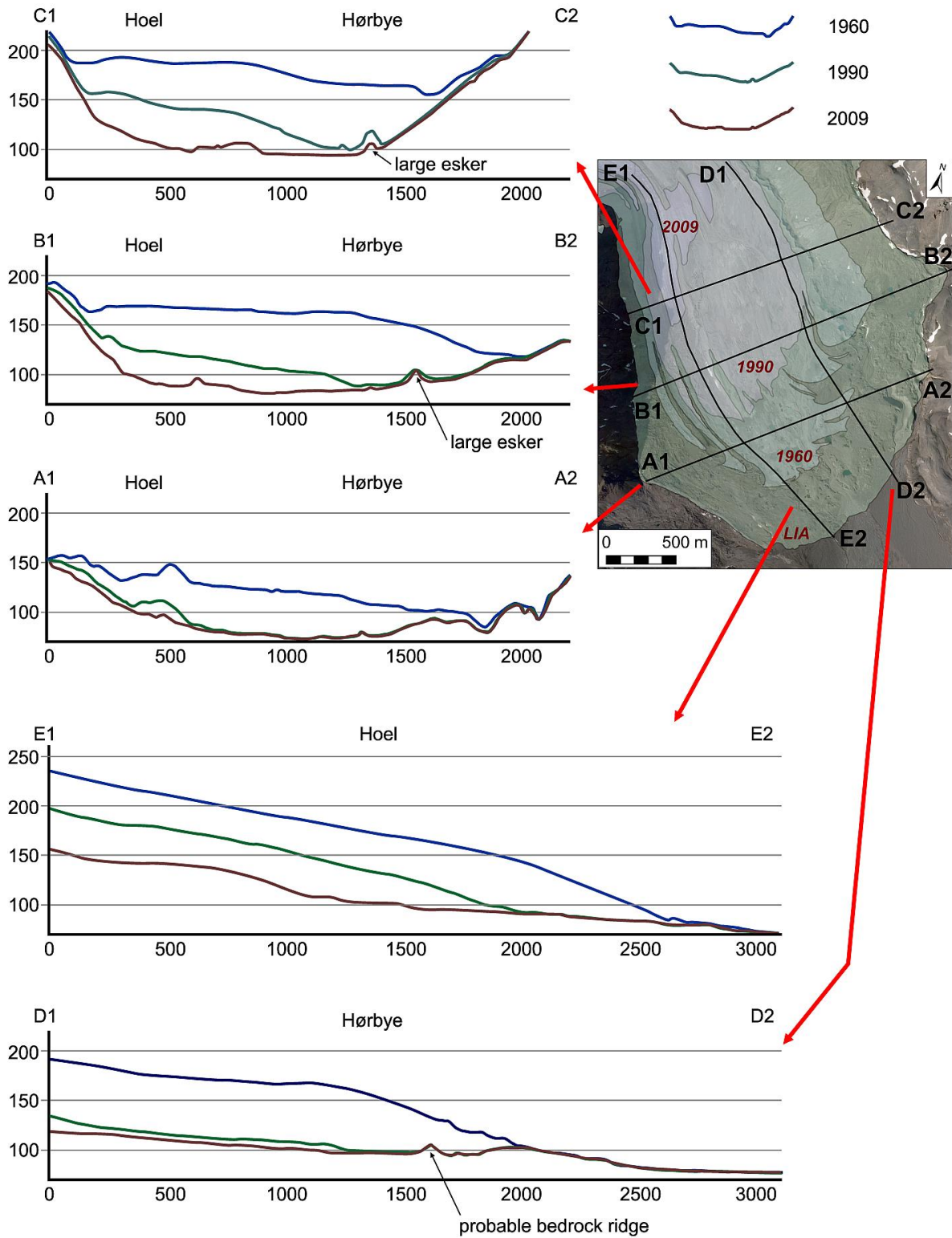




228

229 *Figure 4. (a) Minor exposure of ice-core in the southern lateral moraine resulting from the*  
 230 *development of small debris flow. Note the relatively thin cover of debris protecting moraine*  
 231 *from melting and indicating that this segment of the moraine did not undergo significant*  
 232 *transformations in the past; (b) Cohesive debris flow developed on gentle slopes; (c) Major*  
 233 *exposure of ice-cores in the northern lateral moraine. Note that debris cover is about 1.5-2 m*  
 234 *thick (person for scale) indicating that this part of the moraine was repetitively transformed by*  
 235 *mass movement processes. (d) Retreat of the exposed ice surface from the valley side due to*  
 236 *the emission of heatwave radiation from dark surface of rocks. Note that such separation*  
 237 *seriously limits delivery of fresh debris from valley sides onto glacier surface; (e) Longitudinal*  
 238 *debris stripe – thin and relatively sparse cover of angular debris, which can be traced on the*  
 239 *glacier surface, as well as in the deglaciated foreland overlain on other deposits; (f) Section*  
 240 *through the ice covered by longitudinal debris stripe. Note that even such thin (< 0.1 m) layer*  
 241 *of debris is sufficient to limit ice melting – as a result of differential ablation clean ice surface*  
 242 *visible in the background significantly lowered.*

243



244

245 *Figure 5. Decrease in surface elevation between 1960 and 2009. Longitudinal profiles*  
 246 *demonstrate differences in surface lowering of the Hoel and Hørbye ice flow units, whereas*  
 247 *the transverse profiles show the development of the asymmetric profile of the glacier surface.*



248 The glacier surface long profiles lowered significantly during the period 1961-1990, by as  
249 much as 100 m for the Hørbye ice flow unit. In 1961, the glacier surface showed a characteristic  
250 steep ice front with a mean slope of 11% at the snout contrasting with a flatter up-ice section  
251 of 5% (Figure 5). In 1990, the ice profile of the Hørbye ice flow unit lowered significantly,  
252 indicating a much larger downwasting than frontal recession (volumetric change rather than  
253 aerial change). Between 1990 and 2009, the reduction in elevation of the glacier surface for the  
254 Hørbye ice flow unit was much smaller (10 m) than in the previous period, as most of the ice  
255 had melted and the glacier bed was exposed. In contrast, the Hoel ice flow unit lowered in a  
256 more uniform rate of 50 m in the period 1961-1990 and then another 50 m between 1990 and  
257 2009, but maintaining more or less the same profile shape with a mean slope of 10%.

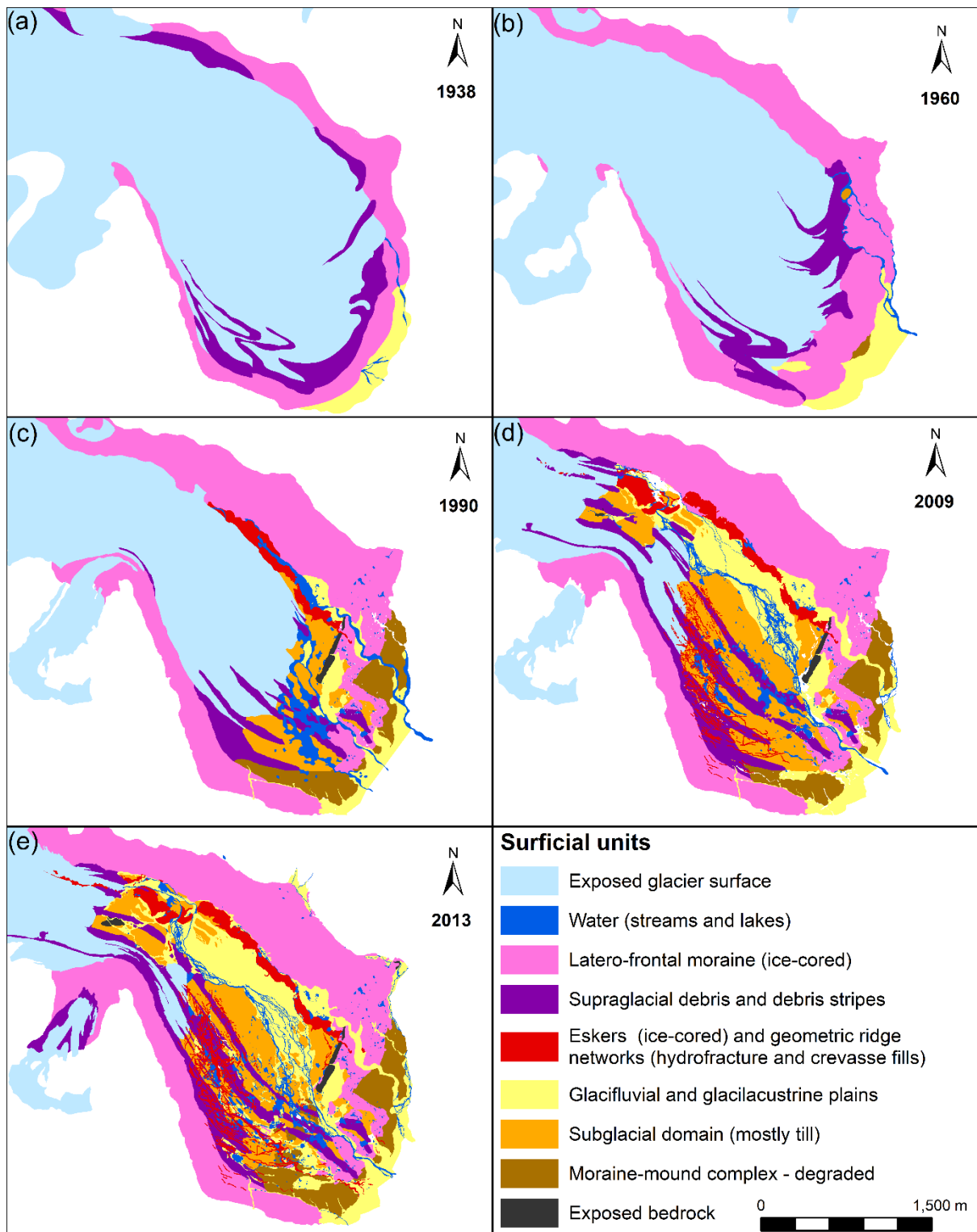
258

#### 259 **4.2. Proglacial (ice-marginal) landform changes LIA - 2013**

260 The area covered by clean glacial ice, ice-cored moraines, till plains, glacifluvial deposits,  
261 rivers and lakes were quantified for each available period for the proximal part of the glacial  
262 system (i.e. between the LIA and the 2013 glacier margins; Fig. 6). The area covered by  
263 different surficial units was used as a proxy for identifying the predominant geomorphological  
264 processes operating over the foreland during the post-LIA period (Fig. 7).

265 In 1938, the ice margin was sited just behind the LIA moraine and hence the exposed glacier  
266 surface was the most dominant surficial unit (Fig. 7). The whole snout was surrounded by  
267 latero-frontal moraines and drainage was not well developed, with the main stream flowing  
268 from the NE part of the ice margin. Supraglacial debris in the form of looped stripes was visible  
269 over the snout (Fig. 6a). There have been no direct historical observations of the glacier surge  
270 that might have been responsible for these looped moraines (cf. Meier and Post, 1969), but  
271 their occurrence potentially indicates that the Hoel ice flow unit surged, or at least advanced  
272 relatively fast, and displaced the Hørbye ice flow unit towards the NE side of the valley.

273 In 1960, due to ice melting and decrease in the elevation of the glacier surface, some of the  
274 supraglacial debris stripes and medial moraines became more visible (Fig. 6b). An increase in  
275 coverage of the unit related to the latero-frontal moraines is also apparent (Fig. 7). Drainage  
276 migrated slightly, with the main stream flowing from the northern part of the ice margin  
277 breaking through the latero-frontal moraine to produce two narrow corridors.

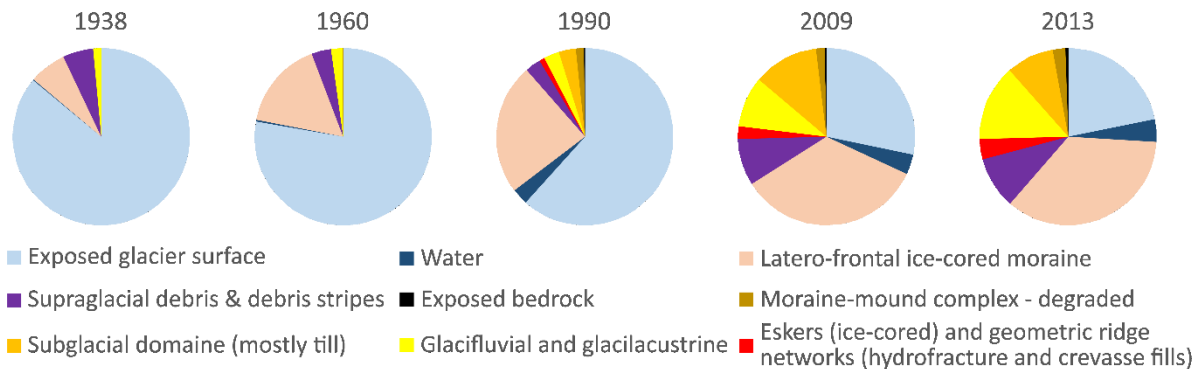


278

279 *Figure 6. Spatio-temporal changes in dominant surficial units and hence process-form regimes*  
 280 *in the snout area and emerging foreland of Hørbyebreen, Svalbard.*

281 In 1990, a further retreat in the glacier margin and lowering of the ice surface resulted in  
 282 exposure of the glacier bed (mostly till) which was visible between the 1990 ice margin and  
 283 the latero-frontal moraines (Fig. 6c). Most parts of these areas were, however, flooded by  
 284 meltwater which was partially blocked by the moraines, creating ponds in front of the ice. Part

285 of the drainage continued along the NE margin using the previously formed corridor, while  
 286 other meltwater pathways developed a new breach in the central section of the latero-frontal  
 287 moraine. Part of the latter was probably de-iced over time, as suggested by characteristic  
 288 landscapes such as kettle-holes and collapsed terrain, and results of previous geophysical  
 289 investigations (cf. Gibas et al., 2005). In the 1990 imagery a large esker ridge became visible  
 290 along the NE margin for the first time. The esker was still ice cored and located above the level  
 291 of the river and outwash, indicating that the esker system was a trace of the previous englacial  
 292 drainage system.



293

294 *Figure 7. Percentage of different surficial units and hence process-form regimes in the snout*  
 295 *and emerging foreland area of Hørbyebreen over time.*

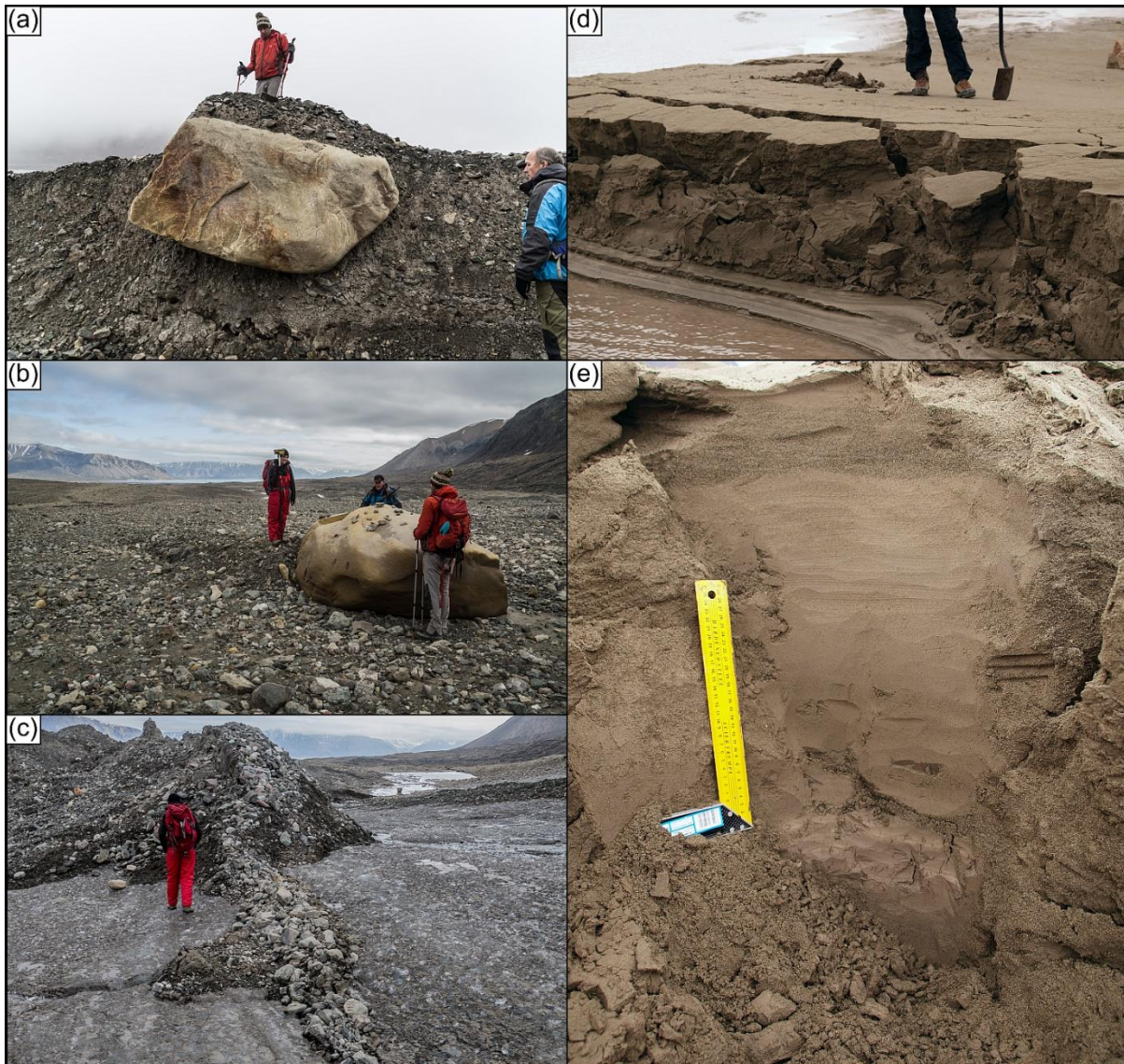
296

297 In 2009, the ice margin was between 1 and 2 km from its maximum extent at the LIA, and  
 298 large-scale reorganization of the foreland had taken place (Fig. 6d). The main meltwater portal  
 299 was still located at the NE part of the margin, but the stream braided through the central part  
 300 of the foreland. It had two consequences: (1) the NE corridor between the esker and later  
 301 moraines was abandoned; (2) most of the meltwater went through the central part of the  
 302 foreland, destroying almost the entire subglacial signature in this area and leaving only small  
 303 patches of subglacial till plain elevated several meters above the outwash level (Fig. 8a, b).  
 304 Degradation of the Hoel ice flow unit had a different character, with ice mostly downwasting  
 305 and developing prominent supraglacial debris stripes overprinted on englacial and subglacial  
 306 geometric ridge networks (crevasse squeeze ridges, hydrofracture infills and small eskers - Fig.  
 307 8c) visible on the SW part of the foreland. Small ponds and streams were also common on this  
 308 part of the foreland.

309 In 2013, ice occupied less than 25% of the foreland (Figure 7), while the ice margin was up to  
 310 3 km from its maximum LIA position (Figure 6e). Further migration of the drainage had taken  
 311 place and had destroyed further subglacial deposits related to the Hørbye ice flow unit. Ice  
 312 marginal retreat also resulted in the exposure of further segments of the ice-cored esker. On  
 313 that part of the foreland occupied by the Hoel ice flow unit, more extensive geometric ridge  
 314 networks were exposed by downwasting ice, together with an increase in the number and size



315 of ponds. Supraglacial debris stripes were still visible and it was possible to trace them in some  
316 places as far as the LIA moraines.



317

318 *Figure 8. (a) Migration of drainage towards the central part of the foreland lead to the*  
319 *destruction of large areas of subglacial deposits. Only small isolated, elevated fragments of*  
320 *subglacial traction tills remained in the northern part of foreland; (b) Larger areas of*  
321 *subglacial deposits temporarily survived in the central part of the foreland but will be probably*  
322 *removed by meltwater in the future. Note small flute hooked behind the boulder. Former ice*  
323 *flow was from lower-right towards middle-left of the picture; (c) Concentration of debris*  
324 *associated with former englacial channel emerging as the ice surface retreated and*  
325 *downwasted; Note that the ridge visible in the picture is still ice-cored; (d) Fine-grained*  
326 *deposits visible after drainage of a short-lived pond in the southern part of the foreland; (e)*  
327 *section through glacial-lacustrine deposits accumulated in short-lived pond, which developed*  
328 *after 1990 and drained before 2009.*

329 The time-series of charts depicting change in surficial unit coverage over time, for an area of  
330 approximately 10 km<sup>2</sup> (Fig. 7), clearly indicate a decrease in importance of process-form  
331 regimes directly related to the ice, along with an increase in the areas covered by glacial  
332 deposits, water bodies and ice-cored moraines (Fig. 7). The area covered by the exposed glacier  
333 ice diminished from 86% in 1938 to about 20% in 2013. As a consequence of glacier retreat  
334 and the evolution of the foreland, areas covered by latero-frontal ice-cored moraines increased  
335 steadily from about 7% in 1938 to more than 35% in 2003. In the period since 1990, most of  
336 the meltwater has flowed through the foreland and the associated glacial processes have  
337 removed a large area of subglacial deposits which have decreased in area from 12% in 2009 to  
338 less than 9% in 2013, concurrent with an increase in glacial deposits to almost 14% in  
339 2013.

#### 340 **4.3. Evolution of the drainage network and pro-glacial lakes, 1936 – 2013**

341 Proglacial streams in front of Hørbyebreen varied over time in terms of location and character  
342 (Fig. 6). For most years, the main meltwater portal at the ice margin was located at the NE side  
343 of the glacier; however, some minor meltwater evacuation portals were also observed in other  
344 sections of the margin.

345 Since 1936, the supraglacial debris cover near the frontal margin of the glacier snout has been  
346 increasingly dissected by small englacial and supraglacial channels. As a consequence, a series  
347 of small esker-like landforms emerged from the SW margin, indicating the former location of  
348 the drainage system to be potentially related to the Hoelbreen ice flow unit. In 1960, minor  
349 streams were no longer visible, and only the largest stream flowed from the NE side of the  
350 Hørbye ice flow unit. This river was still active in 1990 but it migrated laterally, following the  
351 retreat of lateral clean ice margin, and an additional portal was visible where water ponded in  
352 the central part of the foreland between the LIA moraines and 1990 margin. Also visible in  
353 1990 was drainage channelled through the LIA moraines with three ravines being occupied by  
354 active streams, as well as several smaller abandoned corridors. In 2009, the main meltwater  
355 portal was still visible in the northern part of the foreland (more than 3 km from the maximum  
356 ice extent); the main river braided into numerous channels through the foreland, whereas the  
357 northern corridor was abandoned. At the same time, several minor streams flowed from the  
358 Hoel ice flow unit, flowing through a geometric ridge network and thereby creating numerous  
359 shallow ponds in which sedimentation rates were high (Fig. 8d) – based on field observations  
360 thickness of the lacustrine deposits in small ponds formed after 1990 and drained before 2009  
361 was about 0.8 m (Fig. 8e), which equalled to minimum average rate of approximately 2.8  
362 cm/year. In 2013 some further modifications to the drainage were visible but the main  
363 meltwater portal was still located in the north and braiding its way through the foreland, with  
364 minor streams and numerous pond to the south.

365 The clearly developed esker networks reflect a difference in the drainage networks between the  
366 Hørbye and Hoel ice flow units. The Hørbye ice flow unit was drained by a single, large  
367 channel, which led to the development of a large, ice-cored esker along the N and NE side of

368 the glacier. The Hoel ice flow unit was associated with numerous smaller eskers and geometric  
369 ridge networks potentially representing hydrofracture and crevasse infills (Evans et al. 2012).

## 370 **5. DISCUSSION**

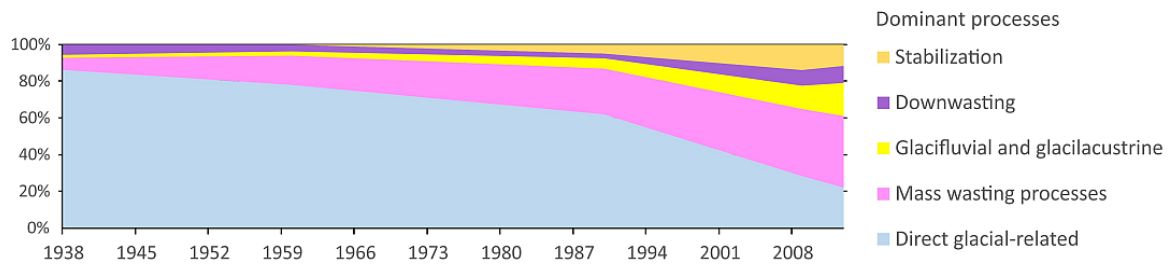
### 371 **5.1. Glacier changes**

372 The historical recession of Hørbyebreen has been far greater than other land-terminating  
373 glaciers located in the vicinity of Petuniabukta (Fig. 1) (Małecki, 2016; Rachlewicz et al.,  
374 2007), with values of 30 and 20 m/year for the Hørbye and Hoel ice flow units respectively  
375 (Fig. 4). The increasing retreat and thinning of the glacier after the LIA indicates that even if  
376 the glacier did surge in the past, it is likely not now capable of accumulating enough mass to  
377 initiate further surges under current climatic conditions (Małecki et al., 2013). This accelerated  
378 retreat has generated a large amount of meltwater, which in turn significantly modified the  
379 glacier foreland over time (see Section 4.3 and Fig. 6). The difference in response between the  
380 Hørbye and Hoel ice flow units is also clearly marked (Fig. 4). If retreat continues in a similar  
381 rate to the present (i.e. 20 – 30 m/year), these two ice flow units will become separate around  
382 the year 2080.

### 383 **5.2. Spatial and temporal changes in the dominant geomorphological processes**

384 The dynamics of the proglacial area of Hørbyebreen illustrate decay in the high-Arctic,  
385 polythermal (had probably surged in the past) glacial landsystem. Using different types of  
386 surficial units as a proxy for the dominant geomorphological processes, five main process-form  
387 regimes were recognized: glacial-related, glacialfluvial and glaciolacustrine, downwasting, mass  
388 wasting processes, and stabilization. Spatio-temporal analysis over the snout area  
389 (approximately 10 km<sup>2</sup>) indicates a serious decrease in processes directly related to the glacier,  
390 i.e. from more than 90% in 1938 to less than 25% in 2013 (Fig. 9). This glacial-related regime  
391 was transformed mostly into one of mass-wasting processes as a result of the development of  
392 large ice-cored lateral moraines. Currently, direct glacial processes have a relatively low impact  
393 on landscape dynamics in proglacial areas. Rather, most of the transformations are related to:

- 394 1) Mass wasting of lateral moraines, where large debris flows develop and lead to  
395 repetitive transformation of landform and sediments (Fig. 4a-c);
- 396 2) Downwasting of dead-ice buried under supraglacial debris, leading to the emergence of  
397 landforms related to the former englacial drainage/crevasse patterns (Fig. 8c);
- 398 3) Glacialfluvial erosion and deposition which effectively removes traces of other processes  
399 and leads to the development of relatively flat, inner outwash plain (Fig. 8a);
- 400 4) Localised glaciolacustrine deposition, leading to rapid accumulation of fine-grained  
401 sediments (cf. Wojciechowski, 1989) (Fig. 8d, e).



402

403 *Figure 9. Changes in dominant processes in the snout and emerging foreland areas of*  
 404 *Hørbyebreen.*

405 In terms of elevation changes, the average lowering of ice-cored lateral moraines in the period  
 406 1960-2009 varied from 0 to 1.5 m/year depending on the local situation. Such values are in the  
 407 same order of magnitude as those of other Svalbard glaciers (Ewertowski, 2014; Ewertowski  
 408 and Tomczyk, 2015; Irvine-Fynn et al., 2011; Midgley et al., 2018; Schomacker and Kjær,  
 409 2008; Tonkin et al., 2016). The remaining part of the proglacial area (approximately 10% in  
 410 2013) was stable over this period and in equilibrium with current climatic and environmental  
 411 conditions. The relatively small size of the stable area compared to other glaciers in the vicinity  
 412 (Ewertowski, 2014; Ewertowski et al., 2016; Ewertowski and Tomczyk, 2015) is related to the  
 413 fact that the drainage of Hørbyebreen has migrated over time and is now impacting upon the  
 414 whole central part of the foreland, destroying large areas of potentially stable geomorphology.

### 415 5.3. Deglaciation scenarios

416 Glacial retreat has resulted in the emergence and paraglacial transformations of a complex  
 417 landform assemblage related to a polythermal glacier snout. Based on field observations and  
 418 the analysis of remote-sensing data, two main domains are identified in the proglacial area of  
 419 Hørbyebreen (Figure 10):

- 420 • **Inner domain related to the temperate ice zone** - In situations where there is a limited  
 421 amount of englacial or supraglacial debris, the final landscape component in the  
 422 foreland will be a subglacial till plain (Fig. 8b). Such till plains are relatively stable, as  
 423 they do not contain dead-ice or steep topography. However, in the case of Hørbyebreen,  
 424 meltwater has destroyed large areas of till plain relatively quickly (Fig. 8a), leading to  
 425 the development of low-lying outwash plains filled with sands and gravels.
- 426 • **Outer domain related to cold-based snout** - Debris concentrations on the ice surface,  
 427 mostly related to medial moraines, controlled moraine or lateral moraines, lead to the  
 428 development of pronounced ice-cored moraine or moraine-mound complexes. Debris  
 429 thickness is initially thin (< 1 m) but enough nevertheless to protect ice from melting  
 430 (Fig. 4a) (cf. Nicholson and Benn, 2006; Nicholson and Benn, 2013). Further  
 431 degradation by debris flows is accelerated by thermal erosion by meltwater and  
 432 repetitive backwasting processes increase the thickness of the debris cover (Fig. 4c).  
 433 Ice-cored moraines are the most active in the period shortly following deglaciation;  
 434 after this initial topographical re-adjustment, thickness of the debris cover is sufficient



435 to almost completely prevent melting of the ice-cores. Further switching between stable  
436 conditions and active degradation depends mostly on local factors (e.g. meltwater,  
437 intensive rainfall, over-steepening of topography due to erosion). When stabilised, such  
438 ice-cored landforms can be stable component of the landscape (e.g. some fragments of  
439 latero-frontal moraine of Hørbyebreen; Fig. 4) over several decades. After final  
440 degradation and de-icing, this depositional scenario results in hummocky topography  
441 with chaotic hills and ponds.

442 This basic scheme was complicated by complex interactions between flow units; and potential  
443 release of pressurised meltwater from temperate parts of the glacier blocked by frozen snout,  
444 which resulted in increasing presence of englacial debris. When debris is concentrated in  
445 various structures within the ice (englacial debris) (Fig. 8c) or as relatively thin longitudinal  
446 debris stripes on the surface of the glacier (Fig. 4e, f), the resultant geomorphology is a complex  
447 pattern of cross-cutting ridges visible in the SW part of the foreland. Such cross-cutting  
448 landforms do not necessarily have a good preservation potential because they contain at least  
449 a certain amount of dead-ice that is partly protected from melting by debris cover. A cross-  
450 cutting planform of ridges favours water ponding, which in turn creates sedimentation traps,  
451 collecting fine-grained glacial-lacustrine material (Fig. 8d, e). Depending on their preservation  
452 potential the final product is usually a landscape that contains low-relief linear hummocks and  
453 small intervening ponds.

454

#### 455 **5.4 Glacial landsystem**

456 Our spatial and temporal analysis of landscape transformations at Hørbyebreen reflects the  
457 downwasting and recession of a high-Arctic polythermal glacier and hence the evolution of the  
458 landsystem signature that is diagnostic of such glaciers. Inherent within this landsystem  
459 evolution is an important switch from direct glacial processes to indirect (paraglacial and  
460 proglacial) processes, the latter being conditioned primarily by ice-core degradation and the  
461 increasing complexity of meltwater drainage networks (Figure 6). Various landform-sediment  
462 assemblages can be identified within the landsystem signature (cf. Evans et al., 2012) and can  
463 be summarized as outer and inner domains typical of the Svalbard polythermal glacial  
464 landsystem (Glasser and Hambrey, 2003). The outer domain relates to the frozen or cold based  
465 snout and comprises the arcuate latero-frontal ice-cored moraine and moraine-mound  
466 complexes, the latter containing variable amounts of buried ice and relating to the formation of  
467 controlled moraine (*sensu* Evans, 2009). The inner domain comprises streamlined (fluted) tills  
468 created in the temperate ice zone that previously lay up-ice from the frozen snout. This simple  
469 zonation is complicated by the interaction of different glacier flow units, especially the  
470 potential surge of the Hoel ice flow unit to form deformed and looped medial moraines, traces  
471 of which are still visible in the landscape. The surge may also have been influential in the  
472 creation of large ice-cored moraines, hummocky terrain and crevasse squeeze ridges (cf. Evans  
473 and Rea, 2003; Evans et al., 2012; Lovell et al., 2018; Lovell et al., 2015; Roberts et al., 2009),  
474 the latter emerging within a dense geometric ridge network that appears to be centred on a zone



475 of linear esker ridges. This landform assemblage comprises small eskers, crevasse-squeeze  
476 ridges and hydrofracture fills and might more realistically relate to the rapid release of  
477 pressurized meltwater from the temperate ice zone of the glacier snout and its injection into the  
478 cold based snout ice rather than surge-induced crevassing. A further azonal domain relates to  
479 the extensive meltwater reworking of landforms and sediments to produce glacial outwash  
480 plains. Finally, the very localized development of glacial lacustrine deposits, especially as they  
481 accumulate over buried glacier ice, is unlikely to result in a significant azonal domain.

482

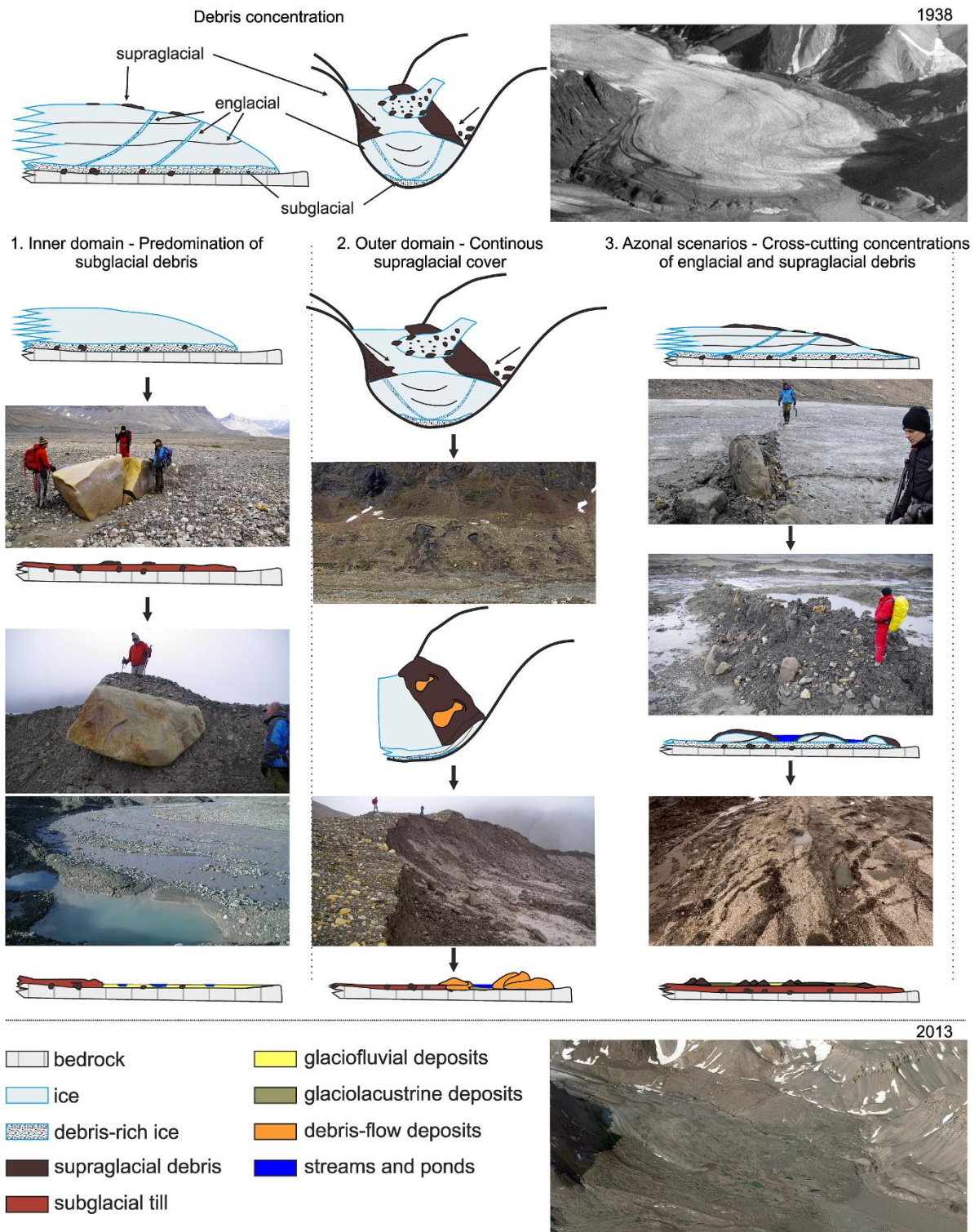


Figure 8. Different scenarios for paraglacial transformation of a complex landform assemblage related to a polythermal glacier snout. Domain zonation and associated debris concentration relates to former distribution of cold-based and temperate ice, and interactions between different flow units. See further explanations in the text.

489 **6. CONCLUSIONS**

490 This study adds data on quantification of multi-decadal scale changes in proglacial landscapes  
491 in the high-Arctic polythermal landsystem by delivering information on planform and  
492 volumetric changes in the foreland of Hørbyebreen, Svalbard. Spatio-temporal analysis of the  
493 foreland of downwasting and retreating Hørbyebreen indicated that:

- 494 1) Area covered by exposed glacial ice between the maximum LIA extent and 2013  
495 decreased from 29.35 km<sup>2</sup> to 16.07 km<sup>2</sup>, which is a reduction in the glacierized area in  
496 the catchment from 62% to 34%;
- 497 2) Total volume loss in proglacial area was 214.9 (+-3%) millions m<sup>3</sup>. This was attributed  
498 mostly to melting of the glacier snout. Degradation of ice-cored landforms was ten  
499 orders of magnitude smaller than of glacier snout.
- 500 3) The transition from areas formerly covered by glacier ice to ice-cored moraines,  
501 glacialfluvial deposits, and other landforms was the most intense in the period 1990-2013.
- 502 4) Former glacier thermal regime and associated volume of debris in englacial and  
503 supraglacial position resulted in the development of two main domains:
- 504 a. Subglacial surfaces related to the inner, temperate ice zone characterised by  
505 former limited englacial and supraglacial debris;
- 506 b. Outer complex of moraine-mounds and arcuate latero-frontal ice-cored moraine  
507 related to the former cold-based snout and large concentration of supraglacial  
508 debris.
- 509 5) Azonal landform assemblages included:
- 510 a. Lopped moraines associated with complex interactions between different flow  
511 units, including potential surge of Hoel flow unit;
- 512 b. Complex geometric ridge network in SW part of the foreland indicating former  
513 surging behaviour or sudden release of pressurised meltwater from temperate  
514 part of the glacier blocked by frozen snout;
- 515 c. Glacialfluvial outwash plains deposited due to lateral drainage migration from  
516 external part of the landsystem to the central part of the foreland.

517 Further investigations into the preservation potential of different landform assemblages are  
518 necessary to fully quantify the impact of future climatic and environmental changes in the  
519 Arctic areas.

520 **References**

- 521 Allaart, L., Friis, N., Ingólfsson, Ó., Håkansson, L., Noormets, R., Farnsworth, W.R., Mertes, J.,  
522 Schomacker, A., 2018. Drumlins in the Nordenskiöldbreen forefield, Svalbard. *Gff*, 1-19.
- 523 Ballantyne, C.K., Benn, D.I., 1994. Paraglacial slope adjustment and resedimentation following recent  
524 glacier retreat, Fåbergstølsdalen, Norway. *Arctic Alpine Res*, 255-269.
- 525 Benn, D.I., Lukas, S., 2006. Younger Dryas glacial landsystems in North West Scotland: an assessment  
526 of modern analogues and palaeoclimatic implications. *Quaternary Sci Rev*, 25(17-18), 2390-  
527 2408.

528 Bennett, G.L., Evans, D.J.A., 2012. Glacier retreat and landform production on an overdeepened  
529 glacier foreland: the debris-charged glacial landsystem at Kvíárjökull, Iceland. *Earth Surf Proc*  
530 *Land*, 37(15), 1584-1602.

531 Bennett, G.L., Evans, D.J.A., Carbonneau, P., Twigg, D.R., 2010. Evolution of a debris-charged glacier  
532 landsystem, Kviarjokull, Iceland. *J Maps*, 40-67.

533 Bennett, M.R., Huddart, D., Glasser, N.F., Hambrey, M.J., 2000. Resedimentation of debris on an ice-  
534 cored lateral moraine in the high-Arctic (Kongsvegen, Svalbard). *Geomorphology*, 35(1-2),  
535 21-40.

536 Bernard, É., Friedt, J., Tolle, F., Marlin, C., Griselin, M., 2016. Using a small COTS UAV to quantify  
537 moraine dynamics induced by climate shift in Arctic environments. *Int J Remote Sens*, 1-15.

538 Błaszczuk, M., Jania, J.A., Kolondra, L., 2013. Fluctuations of tidewater glaciers in Hornsund Fjord  
539 (Southern Svalbard) since the beginning of the 20th century. *Pol Polar Res*, 34(4), 327-352.

540 Boulton, G.S., 1972. Modern Arctic glaciers as depositional models for former ice sheets. *J Geol Soc*  
541 *London*, 128(4), 361-393.

542 Carrivick, J.L., Heckmann, T., 2017. Short-term geomorphological evolution of proglacial systems.  
543 *Geomorphology*, 287, 3-28.

544 Etzelmüller, B., 2000a. On the Quantification of Surface Changes using Grid-based Digital Elevation  
545 Models (DEMs). *Transactions in GIS*, 4(2), 129-143.

546 Etzelmüller, B., 2000b. Quantification of thermo-erosion in pro-glacial areas - examples from  
547 Svalbard. *Z Geomorphol*, 44(3), 343-361.

548 Etzelmüller, B., Hagen, J.O., 2005. Glacier-permafrost interaction in Arctic and alpine mountain  
549 environments with examples from southern Norway and Svalbard. *Geological Society*,  
550 *London, Special Publications*, 242(1), 11-27.

551 Evans, D.J.A., 2009. Controlled moraines: origins, characteristics and palaeoglaciological implications.  
552 *Quaternary Sci Rev*, 28(3-4), 183-208.

553 Evans, D.J.A., Rea, B.R., 2003. Surging glacier landsystem. In: D.J.A. Evans (Ed.), *Glacial Landsystems*.  
554 *Arnold, London*, pp. 259-288.

555 Evans, D.J.A., Strzelecki, M.C., Milledge, D.G., Orton, C., 2012. Hørbyebreen polythermal glacial  
556 landsystem, Svalbard. *J Maps*, 8(2), 146-156.

557 Ewertowski, M.W., 2014. Recent transformations in the high-Arctic glacier landsystem, Ragnarbreen,  
558 Svalbard. *Geografiska Annaler: Series A, Physical Geography*, 96(3), 265-285.

559 Ewertowski, M.W., Evans, D.J.A., Roberts, D.H., Tomczyk, A.M., 2016. Glacial geomorphology of the  
560 terrestrial margins of the tidewater glacier, Nordenskiöldbreen, Svalbard. *J Maps*, 12(sup1),  
561 476-487.

562 Ewertowski, M.W., Kasprzak, L., Szuman, I., Tomczyk, A.M., 2012. Controlled, ice-cored moraines:  
563 sediments and geomorphology. An example from Ragnarbreen, Svalbard. *Z Geomorphol*,  
564 56(1), 53-74.

565 Ewertowski, M.W., Tomczyk, A.M., 2015. Quantification of the ice-cored moraines' short-term  
566 dynamics in the high-Arctic glaciers Ebbabreen and Ragnarbreen, Petuniabukta, Svalbard.  
567 *Geomorphology*, 234, 211-227.

568 Farnsworth, W.R., Ingólfsson, Ó., Retelle, M., Schomacker, A., 2016. Over 400 previously  
569 undocumented Svalbard surge-type glaciers identified. *Geomorphology*, 264, 52-60.

570 Gibas, J., Rachlewicz, G., Szczuciński, W., 2005. Application of DC resistivity soundings and  
571 geomorphological surveys in studies of modern Arctic glacier marginal zones, Petuniabukta,  
572 Spitsbergen. *Pol Polar Res*, 26(4), 239-258.

573 Glasser, N.F., Hambrey, M.J., 2003. Ice-marginal terrestrial landsystems: Svalbard polythermal  
574 glaciers. In: D.J.A. Evans (Ed.), *Glacial Landsystems* *Arnold, London*, pp. 65-88.

575 Gonera, P., Kasprzak, L., 1989. The main stages of development of glacier margin morphology in the  
576 region between Billefjorden and Austfjorden, central Spitsbergen. *Pol Polar Res*, 10(3), 419-  
577 427.

578 Hagen, J., Liestøl, O., 1990. Long-term glacier mass-balance investigations in Svalbard, 1950–88. *Ann*  
579 *Glaciol*, 14, 102-106.

580 Hagen, J., Liestøl, O., Roland, E., Jørgensen, T., 1993. Glacier atlas of Svalbard and Jan Mayen,  
581 Norwegian Polar Institute, Oslo.

582 Hanáček, M., Flašar, J., Nývlt, D., 2011. Sedimentary petrological characteristics of lateral and frontal  
583 moraine and proglacial glaciofluvial sediments of Bertilbreen, Central Svalbard. *Czech Polar*  
584 *Reports*, 1(1), 11-33.

585 Humlum, O., Instanes, A., Sollid, J.L., 2003. Permafrost in Svalbard: a review of research history,  
586 climatic background and engineering challenges. *Polar Res*, 22(2), 191-215.

587 Irvine-Fynn, T.D.L., Barrand, N.E., Porter, P.R., Hodson, A.J., Murray, T., 2011. Recent High-Arctic  
588 glacial sediment redistribution: A process perspective using airborne lidar. *Geomorphology*,  
589 125(1), 27-39.

590 Jania, J., Hagen, J.O., 1996. Mass balance of Arctic glaciers. 5, University of Silesia, Faculty of Earth  
591 Sciences, Sosnowiec-Oslo.

592 Karczewski, A., 1989. The development of the marginal zone of the Hørbyebreen, Petuniabukta,  
593 central Spitsbergen. *Pol Polar Res*, 10(3), 371-377.

594 Karczewski, A., Borówka, M., Kasprzak, L., Kłysz, P., Kostrzewski, A., Lindner, L., Marks, L., Rygielski,  
595 W., Wojciechowska, A., Wysocki, L., 1990. Geomorphology – Petuniabukta, Billefjorden,  
596 Spitsbergen. Adam Mickiewicz University, Poznań.

597 Karczewski, A., Kłysz, P., 1994. Lithofacies and structural analysis of crevasse filling deposits of the  
598 Svenbreen foreland (Petuniabukta, Spitsbergen), XXI Polar Symposium, Warszawa, pp. 123-  
599 133.

600 Karczewski, A., Rygielski, W., 1989. The profile of glacial deposits in the Hörbyedalen and an attempt  
601 at their chronostratigraphy central Spitsbergen. *Pol Polar Res*, 10(3), 401-409.

602 Kellerer-Pirklbauer, A., Proske, H., Strasser, V., 2010. Paraglacial slope adjustment since the end of  
603 the Last Glacial Maximum and its long-lasting effects on secondary mass wasting processes:  
604 Hauser Kaibling, Austria. *Geomorphology*, 120(1), 65-76.

605 Kirkbride, M.P., Deline, P., 2018. Spatial heterogeneity in the paraglacial response to post-Little Ice  
606 Age deglaciation of four headwater cirques in the Western Alps. *Land Degrad Dev*.

607 Kłysz, P., 1985. Glacial forms and deposits of Ebba Glacier and its foreland (Petuniabukta region,  
608 Spitsbergen). *Pol Polar Res*, 6, 283-299.

609 Kociuba, W., 2014. Application of Terrestrial Laser Scanning in the assessment of the role of small  
610 debris flow in river sediment supply in the cold climate environment. *Annales UMCS*,  
611 *Geographia, Geologia, Mineralogia et Petrographia*, 69(1), 79-91.

612 Kociuba, W., 2016. Assessment of sediment sources throughout the proglacial area of a small Arctic  
613 catchment based on high-resolution digital elevation models. *Geomorphology*.

614 Kociuba, W., Kubisz, W., Zagórski, P., 2014. Use of terrestrial laser scanning (TLS) for monitoring and  
615 modelling of geomorphic processes and phenomena at a small and medium spatial scale in  
616 Polar environment (Scott River—Spitsbergen). *Geomorphology*, 212, 84-96.

617 Křížek, M., Krbcová, K., Mida, P., Hanáček, M., 2017. Micromorphological changes as an indicator of  
618 the transition from glacial to glaciofluvial quartz grains: Evidence from Svalbard. *Sediment*  
619 *Geol*, 358(Supplement C), 35-43.

620 Lamplugh, C., 1911. On the shelly moraine of the Sefström Glacier and other Spitsbergen  
621 phenomena illustrative of British glacial conditions. *P Yorks Geol Soc*, 17(3), 216-241.

622 Lefauconnier, B., Hagen, J.O., 1991. Surging and calving glaciers in eastern Svalbard. Oslo.

623 Lønne, I., Lyså, A., 2005. Deglaciation dynamics following the Little Ice Age on Svalbard: Implications  
624 for shaping of landscapes at high latitudes. *Geomorphology*, 72(1-4), 300-319.

625 Lovell, H., Benn, D.I., Lukas, S., Spagnolo, M., Cook, S.J., Swift, D.A., Clark, C.D., Yde, J.C., Watts, T.,  
626 2018. Geomorphological investigation of multiphase glacitectonic composite ridge systems  
627 in Svalbard. *Geomorphology*, 300, 176-188.



628 Lovell, H., Fleming, E.J., Benn, D.I., Hubbard, B., Lukas, S., Rea, B.R., Noormets, R., Flink, A.E., 2015.  
629 Debris entrainment and landform genesis during tidewater glacier surges. *J Geophys Res-*  
630 *Earth*, 120(8), 1574-1595.

631 Lukas, S., Nicholson, L.I., Ross, F.H., Humlum, O., 2005. Formation, Meltout Processes and Landscape  
632 Alteration of High-Arctic Ice-Cored Moraines—Examples From Nordenskiöld Land, Central  
633 Spitsbergen. *Polar Geography*, 29(3), 157-187.

634 Lyså, A., Lønne, I., 2001. Moraine development at a small High-Arctic valley glacier: Rieperbreen,  
635 Svalbard. *J Quaternary Sci*, 16(6), 519-529.

636 Małeckı, J., 2013. Elevation and volume changes of seven Dickson Land glaciers, Svalbard, 1960–  
637 1990–2009. *Polar Res*, 32, 18400.

638 Małeckı, J., 2014. Some comments on the flow velocity and thinning of Svenbreen, Dickson Land,  
639 Svalbard. *Czech Polar Report*, 4(1), 1-8.

640 Małeckı, J., 2016. Accelerating retreat and high-elevation thinning of glaciers in central Spitsbergen.  
641 *The Cryosphere*, 10(3), 1317-1329.

642 Małeckı, J., Faucherre, S., Strzelecki, M.C., 2013. Post-surge geometry and thermal structure of  
643 Hørbyebreen, central Spitsbergen. *Pol Polar Res*, 34(3), 305-321.

644 Meier, M.F., Post, A., 1969. What are glacier surges? *Canadian Journal of Earth Sciences*, 6(4), 807-  
645 817.

646 Mercier, D., Etienne, S., Sellier, D., Andre, M.F., 2009. Paraglacial Bullying of sediment-mantled  
647 slopes: a case study of Colletthogda, Kongsfjorden area, West Spitsbergen (Svalbard). *Earth*  
648 *Surf Proc Land*, 34(13), 1772-1789.

649 Midgley, N.G., Cook, S.J., Graham, D.J., Tonkin, T.N., 2013. Origin, evolution and dynamic context of  
650 a Neoglacial lateral-frontal moraine at Austre Lovénbreen, Svalbard. *Geomorphology*, 198,  
651 96-106.

652 Midgley, N.G., Tonkin, T.N., Graham, D.J., Cook, S.J., 2018. Evolution of high-Arctic glacial landforms  
653 during deglaciation. *Geomorphology*, 311, 63-75.

654 Moholdt, G., Hagen, J.O., Eiken, T., Schuler, T.V., 2010a. Geometric changes and mass balance of the  
655 Austfonna ice cap, Svalbard. *The Cryosphere*, 4(1), 21-34.

656 Moholdt, G., Nuth, C., Hagen, J.O., Kohler, J., 2010b. Recent elevation changes of Svalbard glaciers  
657 derived from ICESat laser altimetry. *Remote Sens Environ*, 114(11), 2756-2767.

658 Nakawo, M., Young, G.J., 1981. Field experiments to determine the effect of a debris layer on  
659 ablation of glacier ice. *Ann Glaciol*, 2, 85-91.

660 Nicholson, L., Benn, D.I., 2006. Calculating ice melt beneath a debris layer using meteorological data.  
661 *J Glaciol*, 52(178), 463-470.

662 Nicholson, L., Benn, D.I., 2013. Properties of natural supraglacial debris in relation to modelling sub-  
663 debris ice ablation. *Earth Surf Proc Land*, 38(5), 490-501.

664 Nuth, C., Kohler, J., König, M., von Deschwanden, A., Hagen, J.O., Kaab, A., Moholdt, G., Pettersson,  
665 R., 2013. Decadal changes from a multi-temporal glacier inventory of Svalbard. *Cryosphere*,  
666 7(5), 1603-1621.

667 Nuth, C., Moholdt, G., Kohler, J., Hagen, J.O., Käab, A., 2010. Svalbard glacier elevation changes and  
668 contribution to sea level rise. *Journal of Geophysical Research: Earth Surface*, 115(F1),  
669 F01008.

670 Östrem, G., 1959. Ice melting under a thin layer of moraine, and the existence of ice cores in  
671 moraine ridges. *Geografiska Annaler*, 41(4), 228-230.

672 Pleskot, K., 2015. Sedimentological characteristics of debris flow deposits within ice-cored moraine  
673 of Ebbabreen, central Spitsbergen. *Pol Polar Res*, 36(2), 125-144.

674 Rachlewicz, G., 2009. Contemporary Sediment Fluxes and Relief Changes in High Arctic Glacierized  
675 Valley Systems (Billefjorden, Central Spitsbergen). Adam Mickiewicz University, Poznań.

676 Rachlewicz, G., 2010. Paraglacial modifications of glacial sediments over millennial to decadal time-  
677 scales in the high Arctic (Billefjorden, central Spitsbergen, Svalbard). *Quaestiones*  
678 *Geographicae*, 29(3), 59-67.

679 Rachlewicz, G., Szczuciński, W., 2008. Changes in thermal structure of permafrost active layer in a  
680 dry polar climate, Petuniabukta, Svalbard. *Pol Polar Res*, 29(3), 261-278.

681 Rachlewicz, G., Szczuciński, W., Ewertowski, M.W., 2007. Post-“Little Ice Age” retreat rates of  
682 glaciers around Billefjorden in central Spitsbergen, Svalbard. *Pol Polar Res*, 28(3), 159-186.

683 Roberts, D.H., Yde, J.C., Knudsen, N.T., Long, A.J., Lloyd, J.M., 2009. Ice marginal dynamics during  
684 surge activity, Kuannersuit Glacier, Disko Island, West Greenland. *Quaternary Sci Rev*, 28(3-  
685 4), 209-222.

686 Schomacker, A., Kjær, K.H., 2008. Quantification of dead-ice melting in ice-cored moraines at the  
687 high-Arctic glacier Holmströmbreen, Svalbard. *Boreas*, 37(2), 211-225.

688 Slater, G., 1925. Observations on the Nordenskiöld and neighboring glaciers of Spitsbergen, 1921.  
689 *The Journal of Geology*, 408-446.

690 Sletten, K., Lyså, A., Lønne, I., 2001. Formation and disintegration of a high-arctic ice-cored moraine  
691 complex, Scott Turnerbreen, Svalbard. *Boreas*, 30(4), 272-284.

692 Staines, K.E.H., Carrivick, J.L., Tweed, F.S., Evans, A.J., Russell, A.J., Jóhannesson, T., Roberts, M.,  
693 2014. A multi-dimensional analysis of pro-glacial landscape change at Sólheimajökull,  
694 southern Iceland. *Earth Surf Proc Land*, n/a-n/a.

695 Stankowski, W., Kasprzak, L., Kostrzewski, A., Rygielski, W., 1989. An outline of morpho-genesis of  
696 the region between Horbyedalen and Ebbadalen, Petuniabukta, Billefjorden, central  
697 Spitsbergen. *Pol Polar Res*, 10, 749-753.

698 Strzelecki, M.C., Long, A.J., Lloyd, J.M., Matecki, J., Zagórski, P., Pawłowski, Ł., Jaskólski, M.W., 2018.  
699 The role of rapid glacier retreat and landscape transformation in controlling the post-Little  
700 Ice Age evolution of paraglacial coasts in central Spitsbergen (Billefjorden, Svalbard). *Land  
701 Degrad Dev*, 29(6), 1962-1978.

702 Strzelecki, M.C., Matecki, J., Zagórski, P., 2015. The Influence of Recent Deglaciation and Associated  
703 Sediment Flux on the Functioning of Polar Coastal Zone–Northern Petuniabukta, Svalbard,  
704 Sediment Fluxes in Coastal Areas. Springer, pp. 23-45.

705 Sund, M., Eiken, T., Hagen, J.O., Kaab, A., 2009. Svalbard surge dynamics derived from geometric  
706 changes. *Ann Glaciol*, 50(52), 50-60.

707 Szuman, I., Kasprzak, L., 2010. Glacier ice structures influence on moraines developement (Hørbye  
708 glacier, Central Spitsbergen). *Quaestiones Geographicae*, 29(1), 65-73.

709 Tonkin, T.N., Midgley, N., Cook, S.J., Graham, D.J., 2016. Ice-cored moraine degradation mapped and  
710 quantified using an unmanned aerial vehicle: A case study from a polythermal glacier in  
711 Svalbard. *Geomorphology*, 258, 1-10.

712 Wheaton, J.M., Brasington, J., Darby, S.E., Sear, D.A., 2010. Accounting for uncertainty in DEMs from  
713 repeat topographic surveys: improved sediment budgets. *Earth Surf Proc Land*, 35(2), 136-  
714 156.

715 Wojciechowski, A., 1989. Sedimentation in small proglacial lakes in the Hörbyebreen marginal zone,  
716 central Spitsbergen. *Pol Polar Res*, 10(3).

717 Zagorski, P., 2011. Shoreline dynamics of Calypsostranda (NW Wedel Jarlsberg Land, Svalbard)  
718 during the last century. *Pol Polar Res*, 32(1), 67-99.

719 Zagorski, P., Gajek, G., Demczuk, P., 2012. The influence of glacier systems of polar catchments on  
720 the functioning of the coastal zone (Recherchefjorden, Svalbard). *Z Geomorphol*, 56, 101-  
721 121.

722 Ziaja, W., 2001. Glacial recession in Sørkappland and central Nordenskiöldland, Spitsbergen,  
723 Svalbard, during the 20th century. *Arctic, Antarctic, and Alpine Research*, 36-41.

724 Ziaja, W., 2004. Spitsbergen landscape under 20th century climate change: Sørkapp Land. *AMBIO: A  
725 Journal of the Human Environment*, 33(6), 295-299.

726 Ziaja, W., 2005. Response of the Nordenskiöld Land (Spitsbergen) glaciers Grumantbreen,  
727 Habergbreen and Dryadbreen to the climate warming after the Little Ice Age. *Ann Glaciol*,  
728 42(1), 189-194.

729 Ziaja, W., Pipala, R., 2007. Glacial recession 2001-2006 and its landscape effects in the  
730 Lindströmfjellet-Håbergnuten mountain ridge, Nordenskiöld Land, Spitsbergen. *Pol Polar*  
731 *Res*, 28(4), 237-247.

732